The EMBO Journal Vol.17 No.8 pp.2177–2185, 1998

Ramifications of kinetic partitioning on usher-mediated pilus biogenesis

E.T.Saulino, D.G.Thanassi, J.S.Pinkner and S.J.Hultgren[1]

Department of Molecular Microbiology and Microbial Pathogenesis, Washington University School of Medicine, 660 South Euclid Avenue, Campus Box 8230, St Louis, MO 63110, USA

[1]Corresponding author
e-mail: hultgren@borcim.wustl.edu

The biogenesis of diverse adhesive structures in a variety of Gram-negative bacterial species is dependent on the chaperone/usher pathway. Very little is known about how the usher protein translocates protein subunits across the outer membrane or how assembly of these adhesive structures occurs. We have discovered several mechanisms by which the usher protein acts to regulate the ordered assembly of type 1 pili, specifically through critical interactions of the chaperone–adhesin complex with the usher. A study of association and dissociation events of chaperone–subunit complexes with the usher in real time using surface plasmon resonance revealed that the chaperone–adhesin complex has the tightest and fastest association with the usher. This suggests that kinetic partitioning of chaperone–adhesin complexes to the usher is a defining factor in tip localization of the adhesin in the pilus. Furthermore, we identified and purified a chaperone–adhesin–usher assembly intermediate that was formed *in vivo*. Trypsin digestion assays showed that the usher in this complex was in an altered conformation, which was maintained during pilus assembly. The data support a model in which binding of the chaperone–adhesin complex to the usher stabilizes the usher in an assembly-competent conformation and allows initiation of pilus assembly.

Keywords: adhesin/chaperone/*Escherichia coli*/pilus/usher

Introduction

A critical virulence mechanism common to most pathogenic bacteria is adherence to host tissues. Initial colonization events have been shown to be crucial in many different infectious processes, e.g. the binding of *Escherichia coli* to Galα(1–4)Gal sugar moieties in the kidney prior to development of pyelonephritis (Roberts *et al.*, 1994). Bacterial adhesins mediate attachment by binding with stereochemical specificity to complementary receptors present on eukaryotic cells. Adhesins can be assembled onto the surfaces of bacteria as monomers, simple oligomers or as parts of supramolecular fibers (Hultgren *et al.*, 1996). The most well-characterized adhesive fibers are known as pili or fimbriae, which are rod-like organelles 5–7 nm in diameter (Mitsui *et al.*, 1973; Hultgren *et al.*, 1996).

Type 1 pili are produced by the entire Enterobacteriaceae family. Their expression requires at least eight genes organized in the type 1 gene cluster (Hull *et al.*, 1981; Orndorff and Falkow, 1984) (Figure 1). Type 1 pili consist of two distinct subassemblies: a thin tip fibrillum which is joined to the distal end of a pilus rod (Jones *et al.*, 1995). The 7 nm wide, 5–7 μm long rod is comprised of FimA subunits arranged in a right-handed helical conformation with 3.125 residues per turn (Mitsui *et al.*, 1973). The tip fibrillum is ~16 Å long and primarily contains the adhesive moiety of the pilus, FimH (Jones *et al.*, 1995). In uropathogenic *E.coli*, FimH mediates binding to mannose-containing receptors (Minion *et al.*, 1989; Krogfelt *et al.*, 1990) exposed on the luminal surface of both the human and mouse bladder epithelium (Langermann *et al.*, 1997). This binding event has been shown to be critical in the ability of uropathogenic *E.coli* strains to colonize the bladder and cause cystitis in mice (Langermann *et al.*, 1997). A FimH-based vaccine has been shown to elicit IgG antibodies that block colonization *in vivo* and protect mice against a mucosal infection of the bladder and subsequent ascending urinary tract infections (Langermann *et al.*, 1997). FimF and FimG have been suggested to play roles in initiation and termination of pilus assembly, respectively (Russell and Orndorff, 1992).

The assembly of >27 different adhesive organelles in diverse Gram-negative bacteria requires a periplasmic chaperone and an outer membrane usher (Hung *et al.*, 1996). FimC is the periplasmic chaperone required for type 1 pilus assembly (Klemm *et al.*, 1992; Jones *et al.*, 1993). It is one of the 27 members of the PapD chaperone family which are 30–60% identical to one another in amino acid sequence (Hung *et al.*, 1996). The crystal structure of PapD, the chaperone involved in P-pilus assembly, has been solved to 2.5 Å resolution. The structure revealed a two-domain boomerang-shaped molecule with each domain having an immunoglobulin-like topology (Holmgren and Brändén, 1989). Molecular modeling revealed that all of the PapD-like chaperones adopt similar immunoglobulin-like two-domain structures (Hung *et al.*, 1996). PapD-like chaperones bind to the C-terminus of subunits via a beta zippering interaction (Kuehn *et al.*, 1993; Bullitt *et al.*, 1996). This interaction results in the partitioning of a subunit from a membrane-associated state to a chaperone-associated periplasmic complex (Jones *et al.*, 1997). The maintenance of the C-terminus of the subunit in an extended conformation in the context of the chaperone may predispose subsequent folding reactions of the subunit on the chaperone template (Jones *et al.*, 1997). Chaperone–subunit complexes are targeted to outer membrane ushers where the chaperone is dissociated. This exposes the conserved C-terminal region which is involved in mediating subunit–subunit interactions within the assembled organelle

(Soto,G., Dodson,K., Liu,C., Jones,C.H., Ogg,D., Knight,S. and Hultgren,S.J., in preparation).

FimD is the outer membrane usher required for type 1 pilus assembly. When *fimD* is disrupted with a Tn*5* insertion, bacteria are unable to produce type 1 pili (Klemm and Christiansen, 1990). Recently it was shown that the usher forms a channel, possibly providing for the translocation of subunits across the outer membrane (Thanassi *et al.*, 1998); however, little is known about the structure, function or mechanism of action of usher proteins. PapC, the usher in the P-pilus system (Figure 1), has been shown to differentially recognize chaperone–subunit complexes relative to the final position of the subunit in the pilus (Dodson *et al.*, 1993). This information has led to the hypothesis that the final position of a subunit in the pilus is determined in part by the strength with which the subunits (complexed with the chaperone) bind to the usher assembly site. The usher is thus a multifunctional protein that presumably has a number of functional regions including membrane-spanning, pore-forming and periplasmic domains. The periplasmic domain presumably interacts with incoming chaperone–subunit complexes. Molecular modeling and topology studies suggest that the FaeD usher has a middle transmembrane portion, and that the N- and C-terminal regions of the protein form periplasmic domains (Valent *et al.*, 1995).

Despite the critical role of pili in colonization and virulence, the usher-mediated mechanism by which bacteria are able to incorporate an adhesin into the pilus is poorly understood. The experiments reported here have uncovered critical chaperone–subunit–usher interactions that have revealed a kinetic partitioning mechanism by which the usher mediates ordered pilus assembly. Due to the almost ubiquitous use of membrane-associated adhesive organelles and secreted proteins by pathogenic bacteria, understanding the events leading to the biogenesis of adhesive organelles and protein translocation across the outer membrane is of fundamental importance. Utilizing the tools we have developed in the type 1 pilus system, we have the unique opportunity to dissect the initial events in the process by which a virulence-associated adhesin is translocated across the outer membrane and incorporated into an adhesive organelle.

Results

Purification and characterization of the usher and chaperone–subunit complexes

A histidine tag was genetically engineered onto the 3′ end of the *fimD* (usher) gene to facilitate purification. This gene product was fully functional *in vivo* as it was able to complement a *fimD*$^-$ type 1 operon (pETS6) using a standard hemagglutination assay (see Materials and methods). The plasmid containing His-tagged *fimD*, pETS4, was transformed into the *type 1*$^-$ strain, ORN103, and protein production was induced. The 92 kDa FimD protein was present in outer membrane preparations as determined by SDS–PAGE (Figure 2A) and N-terminal sequencing. FimD was purified to >90% homogeneity by subjecting the outer membrane preparations to Ni^{2+} chromatography (Figure 2A, lane 5).

A histidine tag was also genetically engineered onto the 3′ end of the *fimC* (chaperone) gene to facilitate purification of chaperone–subunit complexes. The FimC-His tag protein was functional in assembling type 1 pili as it was able to complement a *fimC*$^-$ type 1 operon (pETS12) (see Materials and methods). We transformed the plasmid pETS1000 containing His-tagged *fimC* into

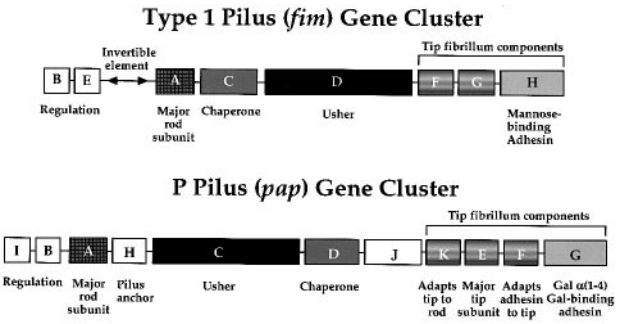

Fig. 1. Schematic representation of the type 1 (*fim*) and P (*pap*) gene clusters listing the functions of the various gene products.

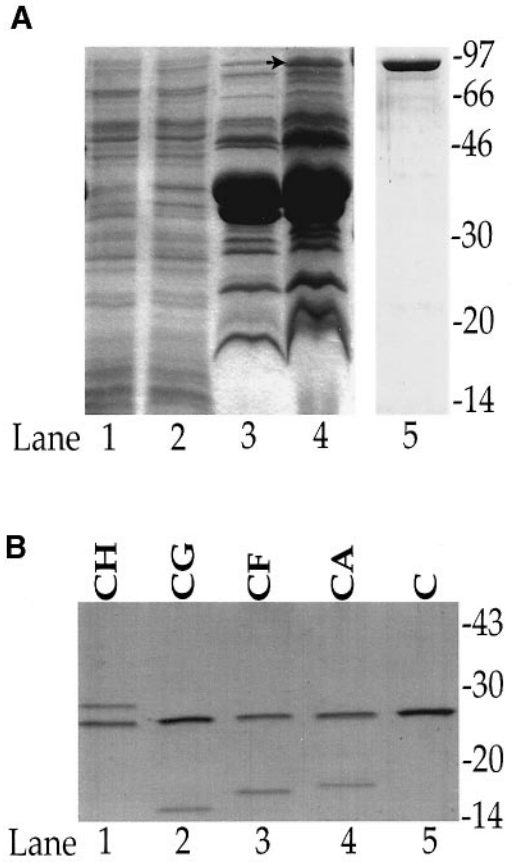

Fig. 2. Purification of usher and chaperone–subunit complexes. (**A**) Coomassie Blue-stained 12.5% SDS–PAGE of ORN103/pETS4 membrane fractions. FimD expression was induced with 20 μM IPTG (lanes 2 and 4). Lanes 1 and 3 are the uninduced controls. Lanes 1 and 2 are inner membrane fractions; lanes 3 and 4 are outer membrane fractions. FimD was only observed in the induced outer membrane fractions (lane 4, arrow). Lane 5 shows FimD purified from the outer membrane extracts by Ni^{2+} chromatography (see Materials and methods). Molecular weight markers in all the figures are in kilodaltons. (**B**) Coomassie Blue-stained 12.5% SDS–PAGE showing the FimC chaperone alone (lane 5), and FimCH (lane 1), FimCG (lane 2), FimCF (lane 3) and FimCA (lane 4) complexes purified by Ni^{2+} chromatography and FPLC as described in Materials and methods.

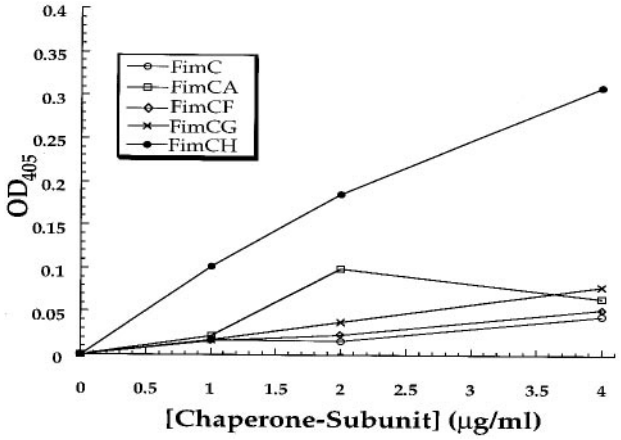

Fig. 3. Chaperone–subunit–usher interactions measured via ELISA. Microtiter plate wells were coated overnight with 5 μg/ml of pure FimD. Wells were blocked with 3% BSA/PBS and then various concentrations of pure FimCA (-□-), FimCF (-◇-), FimCG (-×-), FimCH (-●-), or FimC alone (-○-) were incubated in the wells for 45 min at room temperature. Controls were done with no FimD and with no complexes added (see Materials and methods). Binding to FimD was detected with anti-FimC antibody followed by alkaline phosphatase-linked anti-rabbit IgG. Absorption at 405 nm was read after addition of *p*-nitrophenol phosphate. Points shown represent an average value from experiments done in triplicate.

ORN103 alone or in combination with pETS2A (*fimG*), pETS1 (*fimF*), pHJ20 (*fimH*) or pETS5 (*fimA*). Following protein induction, periplasmic extracts containing chaperone–subunit complexes were subjected to Ni^{2+} chromatography and FPLC. Subunits bound to FimC were co-purified as chaperone–subunit (CH, CG, CF and CA) complexes as determined by SDS–PAGE (Figure 2B). These results reveal that FimC binds to and forms chaperone–subunit complexes with minor subunits (FimG and FimF) and the major subunit (FimA). FimC and FimC–FimH complexes have been identified and purified previously (Jones *et al.*, 1993).

Chaperone–subunit–usher interactions

We used the purified proteins shown in Figure 2 in an enzyme-linked immunosorbent assay (ELISA) to investigate potential interactions between the FimD usher and the chaperone or the various chaperone–subunit complexes. A similar ELISA procedure was performed previously in the study of the PapC usher (Dodson *et al.*, 1993).

FimC–FimH complexes had the highest affinity for FimD (Figure 3). Binding of all of the other complexes and of FimC alone to FimD also occurred, but at a very low level. The strong binding of FimC–FimH complexes to FimD may in part facilitate the localization of the FimH adhesin at the distal end of the tip fibrillum of type 1 pili. This is consistent with the model that Dodson *et al.* (1993) proposed for differential recognition of chaperone–subunit complexes in P-pilus assembly. It is not apparent from the ELISA data what roles might be played by the low level of FimC, FimC–FimG, FimC–FimF and FimC–FimA binding.

Investigation of real time binding events

We reasoned that a study of association and dissociation events in real time would yield additional insight into the ordered mechanism of pilus assembly. Using surface plasmon resonance technology (Karlsson *et al.*, 1991), we attempted to determine both kinetic and equilibrium association and dissociation constants. Using a Biacore 2000 (Biosensor) machine, we immobilized the FimD usher on the surface of a research grade CM5 Biosensor chip using a standard amide cross-linking procedure. Then, we injected various concentrations of purified FimC chaperone or the various chaperone–subunit complexes over the immobilized usher. Representative binding curves for FimCH are shown in Figure 4A. Equilibrium evaluation showed that the FimC chaperone alone was unable to bind to FimD under these experimental conditions. FimCA, FimCG and FimCF bound relatively weakly to the usher, with calculated equilibrium constants (K_D) of 176 nM (FimA), 670 nM (FimCG) and 1.37 μM (FimCF) (Figure 4B). In contrast, chaperone–adhesin (FimCH) complexes bound to FimD 20- to 150-fold better than the other complexes, having a K_D = 9.1 nM. The kinetic basis of the higher affinity of FimCH resided in the k_{on} rate (4.3×10^5 M^{-1} s^{-1}) which was ~8- to 35-fold faster than the k_{on} rates of FimCG, FimCF and FimCA complexes (Figure 4C). In each interaction of the usher with the chaperone–subunit complexes, the k_{off} was very slow, as only ~1.0% of the total number of chaperone–subunit–usher complexes dissociated per second (Figure 4D). Complete pilus assembly occurs in minutes (Jacob-Dubuisson *et al.*, 1994); therefore, in physiological terms, individual chaperone–subunit complexes essentially remain attached to the usher once the initial interaction occurs. The differences in rates of dissociation would not necessarily affect the order of events in pilus assembly because before FimCH could dissociate from FimD, other subunits would presumably be added to FimH, resulting in the growth of a pilus. Accordingly, the ability of FimCH complexes to associate first or fastest with FimD appears to be a critical factor in insuring the tip localization of the FimH adhesin in the pilus.

Biacore binding experiments were also done using the P-pilus system to determine if the principle of a rapid association and slow dissociation of chaperone–adhesin complexes to the usher is a general phenomenon. Analogous to the experiments with the type 1 system, the PapC usher was the immobilized ligand. The binding analytes were the PapD chaperone, a PapDG chaperone–adhesin complex and a chaperone–subunit complex ($PapDA_{G150T}$). PapA subunits make up the pilus rod (Bullitt *et al.*, 1996). The G150T PapA mutant was used because it does not self-aggregate like wild-type PapA (Bullitt *et al.*, 1996). Self-association could possibly interfere with the Biacore analysis. As was found in the type 1 system, the PapDG chaperone–adhesin complex had a 16-fold greater affinity (K_D = 90 nM) (Figure 4B) and a 29-fold faster kinetic rate of association (k_{on} = 5.7×10^4 M^{-1} s^{-1}) (Figure 4C) with the usher in comparison with the $PapDA_{G150T}$ complex. Additionally, the kinetic dissociation rates (k_{off}) remained slow (Figure 4D) and the PapD chaperone alone was unable to interact with the usher (Figure 4B). Therefore, analogous to what was seen in the type 1 pilus system, the faster association rate of the PapDG complex with the PapC usher may play a critical role in enabling the PapG adhesin to take its place as the first subunit incorporated into the pilus. In previous experiments (Dodson *et al.*, 1993), the chaperone–major

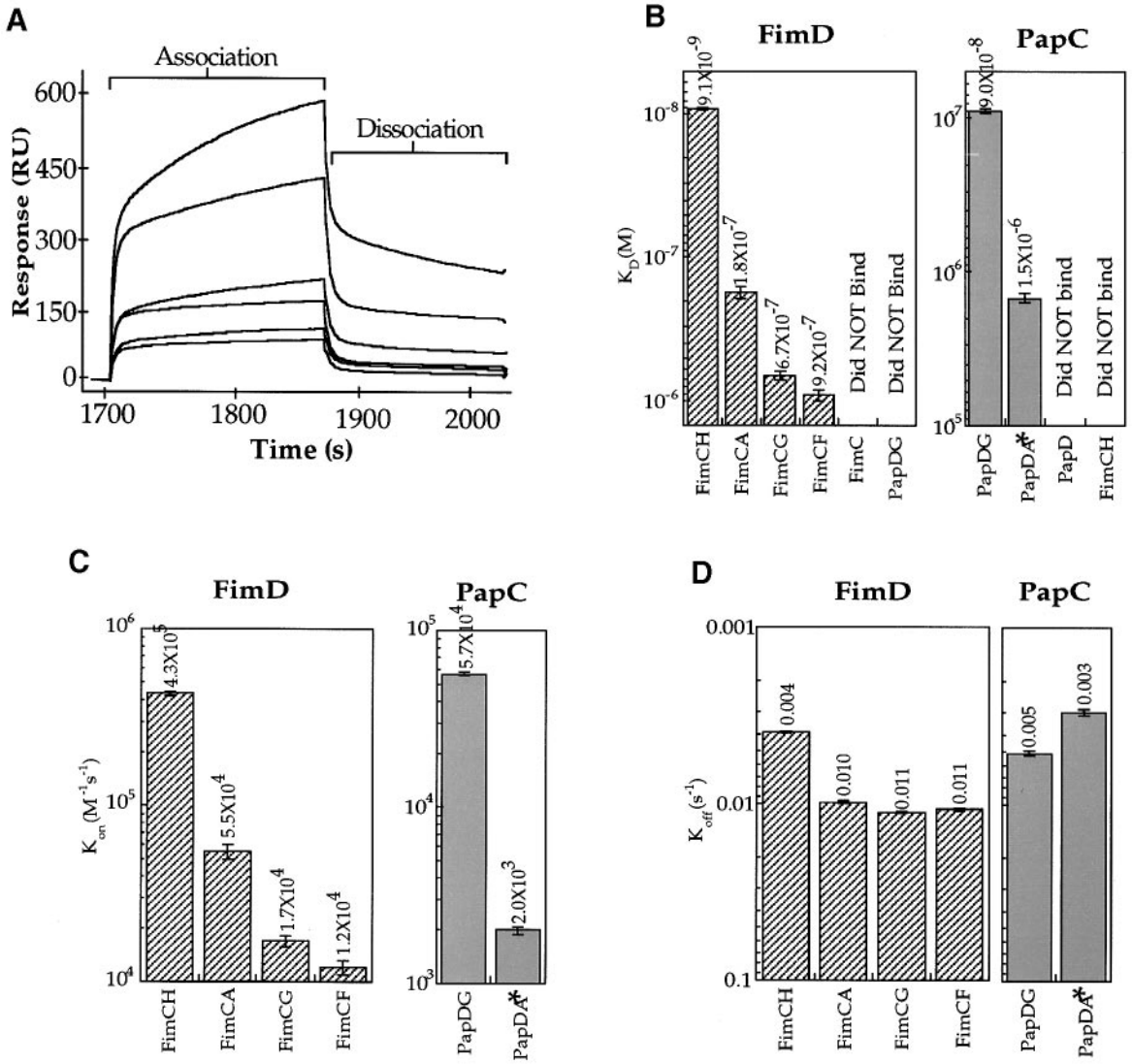

Fig. 4. Real-time analysis of chaperone–subunit–usher interactions. (**A**) Representative binding curves from FimCH–D interactions. The curves (from top to bottom) represent decreasing concentrations of FimCH complex (from 1.0 to 0.075 μM) injected over immobilized FimD. Binding of FimCH to FimD is detected by the Biacore machine and converted to an arbitrary response unit (RU) over time (s) that can be analyzed to obtain kinetic and equilibrium constants. The regions representing real-time association and dissociation events are labeled. (**B**) Log scale graphs showing equilibrium dissociation constants (K_D in molar concentration units) for various chaperone–subunit–usher interactions in the type 1 (left graph) and P-pilus (right graph) systems. For (B–D), the numbers listed above each bar in the graph represent the actual binding constant for that particular chaperone–subunit complex. The columns labeled PapDA* represent experiments done with $PapA_{G150T}$ (Bullitt *et al*., 1996) complexed with PapD. Standard errors shown graphically for k_{off} and k_{on} are an average of the standard errors from all measurements taken for a particular complex. The standard error for K_D is a combination of the errors from the k_{off} and k_{on} (see Materials and methods). The chaperone–adhesin (FimCH or PapDG) complex in each system bound to the usher with a much greater affinity than any of the chaperone–subunit complexes. The chaperone alone (FimC or PapD) did not show any binding to the usher (FimD or PapC, respectively) when injected (up to 10.0 μM). The chaperone–adhesin complex (PapDG or FimCH) that was 'mismatched' (to FimD or PapC, respectively) also did not show any binding when injected (up to 2.0 μM). (**C**) Log scale graphs showing kinetic association constants (k_{on} in M^{-1} s^{-1}) for type 1 and P-pilus systems. The chaperone–adhesin complexes in both systems bound fastest. (**D**) Log scale graphs showing kinetic dissociation constants (k_{off} in s^{-1}) for type 1 and P-pilus systems. The 'off' rate is slow for all of the complexes (~1% of the complexes dissociating per second).

subunit complex (PapDA) was not shown to bind to the usher (PapC). The fact that we were able to detect binding of PapDA and of FimCA to their respective ushers (Figure 4B) is probably due to the use of pure protein and to the increased sensitivity of the surface plasmon resonance technique. The inability to detect binding of the chaperone alone or the mismatched chaperone–adhesin complex to the usher (Figure 4B) argues that even the weak interactions observed are biologically relevant.

Changes in trypsin susceptibility of FimD upon FimCH binding

Next, we wanted to determine if usher–chaperone–subunit interactions could be detected *in vivo*. We hypothesized that these interactions might result in conformational changes in the usher which could be detected by differences in sensitivity to trypsin. This assay was used successfully for studying surface-exposed loops and mapping the topology of the K88 usher, FaeD (Valent *et al.*, 1995).

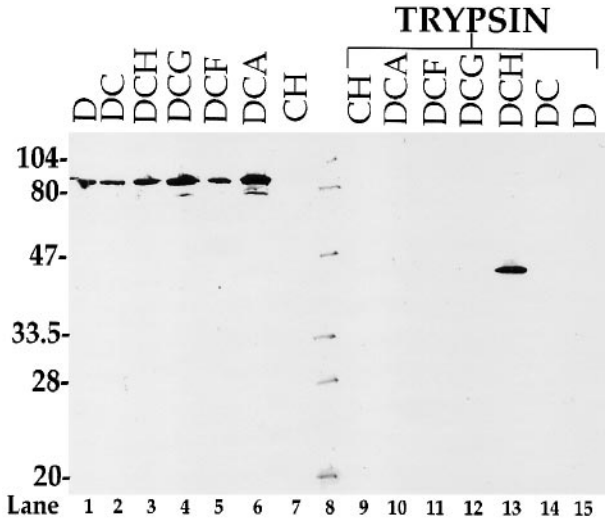

Fig. 5. Susceptibility of FimD to cleavage by extracellular trypsin. The presence of FimD in outer membrane extracts was analyzed by Western blotting with anti-FimD antiserum before (lanes 1–7) or after (lanes 9–15) the cells were treated with trypsin. Lane 8 shows molecular weight markers. FimD was expressed by itself (lanes 1 and 15) or co-expressed with FimC (lanes 2 and 14), FimCH (lanes 3 and 13), FimCG (lanes 4 and 12), FimCF (lanes 5 and 11) or FimCA (lanes 6 and 10). As a negative control, FimCH alone was expressed (lanes 7 and 9). The N-terminal sequence of the trypsin-protected portion of FimD (lane 13) was FTDYYN. This placed the trypsin cleavage site at K477 of the mature protein.

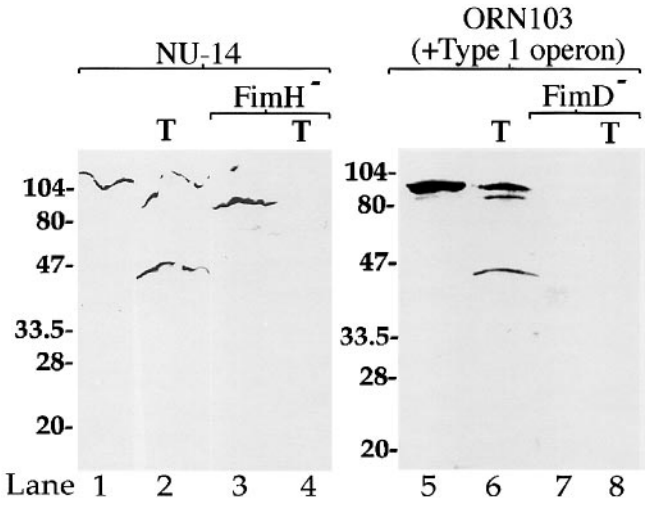

Fig. 6. Trypsin susceptibility of FimD in cells producing pili. Outer membrane preparations of piliated NU14 or NU14-1 (*fimH*⁻) cells (left gel) or ORN103 cells containing the type 1 pilus operon [pSH2 or pETS6 (*fimD*⁻)] (right gel) were analyzed for the presence of FimD by Western blotting with anti-FimD antiserum before (lanes 1, 3, 5 and 7) or after (lanes 2, 4, 6 and 8) the cells were treated with trypsin. The abnormally wavy pattern of FimD migration (lanes 1–4) is probably due to the presence of wild-type lipopolysaccharide in the clinical strain NU14. The different mobility of FimD in NU14 (lane 1) versus FimD in NU14-1 (lane 3) may be due to the assembly state of the usher as pili are being assembled in NU14 but not in NU14-1 (Langermann *et al.*, 1997).

Trypsin digestion of whole cells expressing the FimD usher alone or co-expressed with either FimC, FimCF, FimCG, FimCH or FimCA was followed by Western blotting of outer membrane preparations using anti-FimD antiserum (Figure 5). When FimD was expressed alone or with FimC, FimCF, FimCG or FimCA individually, it was susceptible to complete proteolytic degradation by trypsin under the conditions used. It was somewhat surprising to find the outer membrane usher protein to be completely susceptible to externally added trypsin. This indicates that FimD must have a high number of surface-exposed trypsin-cleavable sites or that cleavage at one or a few sites leads to destabilization and further degradation of the protein. However, as seen in Figure 5, lane 13, a large portion of the FimD usher was protected from proteolytic digestion when the chaperone–adhesin complex, FimCH, was co-expressed. The same results were obtained when whole cell suspensions were probed by Western blot analysis (data not shown), arguing that additional digestion did not occur during preparation of the outer membranes. The FimD fragment protected by co-expression of FimCH was purified by Ni^{2+} chromatography (Figure 7) and N-terminally sequenced, demonstrating that it represents a 40 kDa C-terminal domain of FimD beginning with amino acid K477 of the mature protein. Cleavage occurred in an extracellular region of FimD, because the periplasm was not accessible to trypsin in these whole cell experiments. This was confirmed by showing that the periplasmic FimC chaperone, which is trypsin-sensitive (unpublished data), was not cleaved by trypsin in this experiment (data not shown). Finally, if we lowered the concentration of trypsin or decreased the digestion time, a small amount of this protected 40 kDa fragment could be seen in an anti-FimD Western blot even

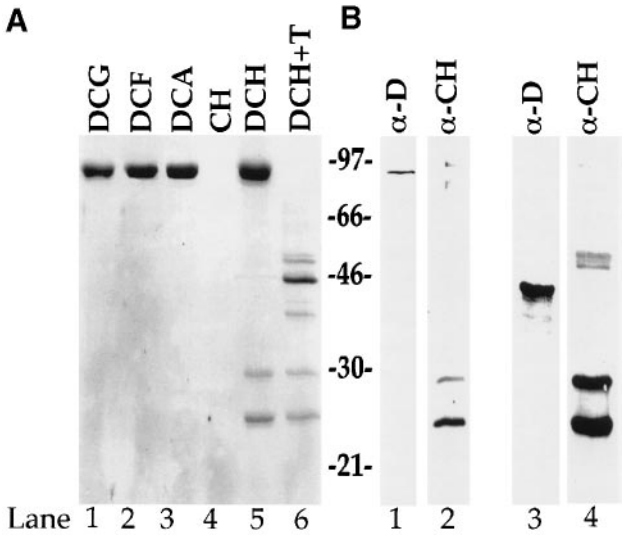

Fig. 7. Purification of the ternary FimC–FimH–FimD assembly intermediate. (**A**) Coomassie Blue-stained 12.5% SDS–PAGE of outer membrane preparations after Ni^{2+} chromatography. The preparations were from cells in which His-tagged FimD (from pETS4) was co-expressed with non-His tagged FimCG (lane 1), FimCF (lane 2), FimCA (lane 3) or FimCH (lane 5). Lane 4 shows that non-His-tagged FimCH alone does not stick to Ni^{2+} beads. Lane 6 shows that the 40 kDa C-terminal fragment protected from extracellular trypsin digestion can be purified by Ni^{2+} chromatography as a ternary complex with FimCH. (**B**) Western blots of the FimD–FimC–FimH complex eluted as a single peak from a Superdex 200 column after Ni^{2+} chromatography and developed with anti-FimD (lanes 1) or anti-FimCH (lanes 2) antibodies. Western blot of an extract from trypsin-treated cells identical to that shown in (A), lane 6, developed with anti-FimD (lane 3) or anti-FimCH (lane 4).

when FimD was expressed by itself or with any of the other Fim proteins (data not shown). This suggests that the FimD usher may exist in an equilibrium between protected and unprotected conformations, and that interaction of FimCH with FimD drives the usher into the protected form.

We next investigated whether the trypsin-protected form of FimD induced by interaction with the FimCH complex is maintained throughout pilus biogenesis. The state of type 1 pilus-assembling FimD was investigated using ORN103 cells containing the plasmid pSH2, which carries the entire type 1 operon (Orndorff and Falkow, 1984), or pETS6, a FimD knock-out of pSH2 that does not produce pili (unpublished data). We also used the clinical isolate NU14 (Hultgren *et al.*, 1986) and a *fimH*$^-$ mutant of NU14, NU14-1 (Langermann *et al.*, 1997). The cells were grown under conditions that resulted in the expression of type 1 pili, as confirmed by their ability to hemagglutinate guinea pig erythrocytes (see Materials and methods), and then subjected to the trypsin treatment described above. In all cases, the 40 kDa portion of the FimD usher that was protected by the co-expression of FimCH was also protected during expression of type 1 pili (Figure 6). This indicates that the conformation of the usher that is stabilized by its interaction with the chaperone–adhesin complex is maintained throughout pilus assembly. It should be noted that in these experiments a substantial portion of full-length FimD remained undigested by trypsin. This could be due to steric inhibition of the protease by the 7 nm wide pilus rod.

Isolation of a FimD–FimC–FimH assembly intermediate formed in vivo

The values derived from the Biacore experiments suggest a strong and long-lasting interaction between FimCH and FimD, and the trypsin digestion results show that this interaction occurs *in vivo*. Therefore, we attempted to isolate a pilus assembly intermediate targeting the step at which the FimD usher interacts with FimC–FimH complexes. We co-expressed His-tagged FimD (pETS4) with non-His-tagged FimC and FimH (pETS1004) in ORN103 cells, and purified FimD using Ni^{2+} chromatography as discussed above. We found that FimC and FimH co-purified with FimD, suggesting a stable, ternary, usher–chaperone–adhesin (FimD–FimC–FimH) complex (Figure 7A, lane 5). Non-His-tagged FimCH complexes expressed in the absence of FimD could not be purified by Ni^{2+} chromatography (Figure 7A, lane 4). This is the first demonstration of the *in vivo* formation of an usher intermediate in pilus assembly. When FimCA, FimCG or FimCF were co-expressed with FimD, none of these chaperone–subunit complexes co-purified with the usher (Figure 7A, lanes 1–3), consistent with their weak interactions as seen in the Biacore experiments and their inability to protect FimD from trypsin. The putative FimD–FimC–FimH complex was analyzed by FPLC gel filtration chromatography (Superdex 200) and was shown to elute as a single peak (Figure 7B, lanes 1 and 2).

The sensitivity of the ternary complex to trypsin was also analyzed. We co-expressed the FimD usher with FimCH and subjected the cells to the tryptic digestion reaction as discussed above. The outer membrane fraction was then subjected to Ni^{2+} chromatography which resulted in the co-purification of the 40 kDa C-terminal fragment of FimD with FimCH (Figure 7A, lane 6, and B, lanes 3 and 4). These data demonstrates that the probable binding site for the FimCH chaperone–adhesin complex is in the C-terminal portion of FimD.

Discussion

Presentation of a pilus-bound adhesin protein for optimal binding to eukaryotic cells is a critical event in bacterial pathogenesis (Roberts *et al.*, 1994; Langermann *et al.*, 1997). The assembly of >27 diverse adhesive fibers in many different Gram-negative bacteria occurs via a multistep chaperone–usher pathway (reviewed in Hultgren *et al.*, 1996). In the terminal step, protein subunits are translocated across the outer membrane and assembled into composite heteropolymeric organelles in a defined order. The translocation event depends on the outer membrane usher. The usher forms an oligomeric assembly that spans the outer membrane and has an ~2 nm channel (Thanassi *et al.*, 1998). The pilus subunits are maintained in assembly-competent native-like conformations on the periplasmic chaperone template as they are escorted to the outer membrane ushers. Presumably, these chaperone–subunit complexes specifically interact with a periplasmic domain on the usher. Subsequent events result in the exchange of subunit–chaperone interactions for subunit–subunit interactions that may drive the assembly of the pilus.

Utilizing Biacore 2000 technology to examine 'real time' interactions, we discovered that the FimCH chaperone–adhesin complex bound to the FimD usher with a 20- to 150-fold higher affinity and with an 8- to 35-fold faster kinetic association rate (k_{on}) than the other chaperone–subunit complexes. The kinetic dissociation rates (k_{off}) of all of the complexes were found to be physiologically slow, arguing that the targeting of FimCH first or fastest to FimD is a critical factor in determining the position of the FimH adhesin at the tip of the pilus. The slow dissociation rates may also be part of a kinetic partitioning mechanism to ensure that subunits are incorporated into pili subsequent to their interaction with the usher. We found that the same kinetic partitioning existed in the P-pilus system, and thus it may represent a conserved mechanism in many or all of the chaperone–usher pathways to regulate the ordered assembly of adhesive organelles. It is uncertain to what extent kinetic partitioning may regulate the later steps in ordered assembly.

The interaction between the FimCH chaperone–adhesin complex and the usher, FimD, evidently represents a critical event in the assembly of the type 1 pilus. In the NU14 clinical isolate, a *fimH*$^-$ mutation (NU14-1) nearly abolishes pilus assembly (Langermann *et al.*, 1997). This effect has also been observed in another clinical isolate (Connell *et al.*, 1996). We show here that interaction of the FimCH complex with FimD most likely transduces a conformational change to surface-exposed regions of FimD, making them trypsin resistant. This conformational change is maintained throughout pilus assembly. In the *fimH*$^-$ NU14-1 strain, the inability of the usher to adopt a trypsin-resistant conformation may explain the lack of pili produced by this and other *fimH*$^-$ mutant strains. Therefore, we suggest that the FimCH interaction

primes the usher for pilus assembly by driving it into an assembly-competent conformation. However, there are reports suggesting that *ΔfimH* laboratory strains can produce pili (although at reduced levels) (e.g. Maurer and Orndorff, 1985; Klemm and Christiansen, 1987). This could be explained by a dynamic usher protein which, particularly in laboratory strains, exists in a conformational equilibrium between assembly-competent and -incompetent states. Indeed, under less stringent conditions, we found that in the ORN103 lab strain, a small amount of the trypsin-protected form of FimD is present even in the absence of FimCH. Our data clearly show, however, that the FimC–H–D interaction stabilizes the protected conformation of FimD, locking the FimD usher into a conformation that is capable of mediating pilus assembly. In their topological study of the K88 pilus usher, FaeD, Valent *et al.* (1995) observed that an ~45 kDa portion of the usher was protected from extracellular trypsin digestion even though no chaperone-subunit complexes were co-expressed. A more complete degradation of the FaeD usher may not have been seen for a number of reasons. For example, there may be differences in the lengths of surface-exposed loops and/or trypsin cleavage sites. Valent *et al.* (1995) did not investigate the effects of individual chaperone–subunit interactions with the FaeD usher and, therefore, it is unknown whether these interactions would confer altered protease susceptibility to FaeD.

An alternative explanation for the trypsin resistance conferred to FimD by co-expression of FimCH is that the FimH adhesin becomes translocated to the cell surface where it sterically inhibits trypsin cleavage of the FimD usher. However, this does not appear to be the case. Using anti-FimH antibodies in an immunogold electron microscopy procedure, we were unable to detect FimH on the surface of ORN103-containing pETS4 (fimD)/pETS1001 (fimCH) and these cells were hemagglutination negative (data not shown). This argues that under conditions when only FimC, FimH and FimD are expressed, FimH is not translocated across the outer membrane.

The data presented here suggest the following model. After the FimCH chaperone–adhesin complex binds to the periplasmic C-terminal domain of the FimD usher, it forms a stable ternary complex that results in a conformational change in the usher. This ternary complex, which is formed more quickly than any other usher–chaperone–subunit complex, probably acts as an 'assembly initiation complex', providing a template for the next incoming chaperone–subunit complex (FimCG) and locking FimD into an assembly-competent state. There is no evidence that the interaction of FimCH with FimD results in an uncapping of the chaperone (FimC) from the adhesin (FimH). Interaction of the incoming FimCG complex with the FimC–H–D ternary complex would then result in uncapping of the chaperone, via an exchange of a FimH–FimC interaction for perhaps a more favorable FimH–FimG interaction. In the P-pilus system, it has been shown that the chaperone binds to a highly conserved beta zipper motif at the C-terminus of subunits (Kuehn *et al*., 1993). This same motif participates in subunit–subunit interactions after the uncapping of the chaperone (Bullitt *et al*., 1996). FimC has a similar mechanism of action to that of PapD (Jones *et al*., 1993). Thus, a surface on the tip fibrillum subunit, FimG, not capped by the chaperone probably fits to a complementary surface on FimH; however, that surface on FimH remains capped by the chaperone in the ternary FimCH–FimD complex. Uncapping of the chaperone from the C-terminal beta zipper of FimH allows the FimG–FimH assembly interaction to occur. The C-terminal beta zipper of FimG would then remain capped by the FimC chaperone until the next subunit (FimF) is added to the growing pilus. FimH–FimG–FimF–FimC assembly intermediates have been identified previously (Jones *et al*., 1995), demonstrating the feasibility of such a model.

We feel that the experiments presented here elucidate critical interactions in the biogenesis of type 1 pili. By understanding the roles that the usher FimD, the chaperone FimC and the adhesin FimH are playing in type 1 pilus biogenesis, we believe that a more generalized understanding of the events responsible for translocation across the bacterial outer membrane may be realized. The requirement for translocation of a protein across the outer membrane is not unique to the 27 known chaperone–usher pathways. Instead, this represents a common theme in many other secretory machineries such as the type II secretion system which is involved in the secretion of virulence factors and the biogenesis of type IV pili (Salmond, 1996), the type III secretion system which is involved in the injection of virulence factors into host cells in a wide variety of bacteria (Lee, 1997) and even the production of filamentous phage (Russel, 1995). There is very little known about how any of the proteins from these various systems cross the outer membrane although all have requisite usher-like outer membrane proteins to serve in translocation (Kazmierczak *et al.*, 1994; Salmond, 1996; Lee, 1997). In fact, similarities in higher order structure between these outer membrane proteins and ushers have begun to emerge (i.e. Linderoth *et al*., 1997; Bitter *et al.*, 1998; Thanassi *et al*., 1998). Understanding the details of secretion across the outer membrane in the type 1 pilus system may reveal strategies for targeting these various machineries in the design of novel antimicrobial agents that block the assembly or secretion of virulence factors.

Materials and methods

Plasmids and strains

The *E.coli* strain ORN103 was described previously (Orndorff and Falkow, 1984) as were strains NU14 and NU14-1 (Hultgren *et al.*, 1986; Langermann *et al*., 1997). All restriction and DNA-modifying enzymes were from New England Biolabs. Plasmid pAN2 was made by taking a fragment of pSH2 containing *fimD* and placing it into pMMB91 (Dodson *et al.*, 1993). In order to produce His-tagged FimD, a portion of *fimD* was taken from pAN2 and cloned into pBR322 (pFimDtr). Then a PCR-generated fragment containing the coding region from the *Pvu*I site of *fimD* to the 3′ end of the gene, along with the addition of six histidine codons and a *Pst*I site, was cloned into the *Pvu*I and *Pst*I sites in pFimDtr. The *fimD* gene with the six additional histidine codons was removed and ligated into pMMB66 (Furste *et al.*, 1986) giving pETS4. pETS1000 was made by cloning a PCR-generated fragment containing the coding region of *fimC* from the *Nsi*I site to the 3′ end with the addition of six histidine codons and an *Xba*I site into *Nsi*I–*Xba*I-cut pHJ9205 (Jones *et al.*, 1995). pETS1 was made by cutting *fimF* from pSH2 and cloning the fragment into pACYC184, making pFimF. After ensuring proper orientation, *fimF* was cut from pFimF and ligated into pMMB91, completing pETS1. The *fimG* gene was isolated by cutting *fimG* from pSH2 and ligating the fragment into pMMB66, making pETS2A. Inducible FimA production was ensured by using PCR to generate the *fimA* gene with an *Eco*RI site at the 5′ end and a *Bam*HI sites at the 3′ end of the gene. The PCR fragment was cloned into those

sites in pMMB66, making pETS5. pETS1001, pETS1002, pETS1003 and pETS1005 were made by cutting pHJ20, pETS2A, pETS1 or pETS5 and ligating into pETS1000. pETS1004 was made in the same way as the other pETS100N constructs except that the fragment was ligated into pHJ9205 instead of pETS1000. Correct orientation was checked by restriction enzyme digest and protein production for all. All of the PCR fragments mentioned above were sequenced to ensure fidelity. The *fimD* knock-out in the plasmid-encoded type 1 operon, pETS6, was made by digesting pSH2 with *Pvu*I, blunting with T4 DNA polymerase and partially digesting with *Eco*RI. A gene fragment corresponding to the 3′ end of *fimC* was cut from pHJ9205 and the fragment was ligated with the fragment of pSH2, giving pETS6 which contains all of the type 1 genes but is missing ~2.3 kb at the 5′ end of *fimD*. ORN103 transformed with pETS6 and pMMB66 could not hemagglutinate guinea pig red blood cells, while cells with pETS6/pETS4 gave HA titers that were equal to that of ORN103 containing pSH2 (1:128 compared with a titer of 0 with pETS6/pMMB66). A plasmid containing an isopropyl-β-D-thiogalactopyranoside (IPTG)-inducible *fimC*$^{-}$ operon was made using pETS5 with a fragment ligated in from pSH2 that contained *fimFGH*. A fragment from this new plasmid containing *fimAFGH* was ligated into pETS4, giving pETS12. The pETS12 plasmid in ORN103 gave no HA titer but could be complemented with either pETS1000 or pHJ9205 to give HA titers that were equivalent to pSH2.

Isolation and purification of FimD and FimC–subunit complexes

ORN103 cells transformed with pETS4 were grown at 37°C with aeration to an OD_{600} of ~0.6, and FimD production was induced with 10 μM IPTG for 1 h. The cells were harvested by centrifugation, washed once with 20 mM HEPES (pH 7.5), passed twice through a French Press (American Instrument Co.), and the membrane fraction collected by centrifugation at 100 000 *g* for 1 h. The membrane fraction was solubilized by resuspending in 20 mM HEPES (pH 7.5) and Sarkosyl solution at room temperature, followed by centrifugation at 100 000 *g* for 1 h. This resulted in essentially only outer membrane components in the pellet. For Ni^{2+} chromatography purification, the outer membrane was solubilized by rocking at room temperature in a 1.0% Elugent (Calbiochem)/20 mM HEPES (pH 7.5) solution for 1 h followed by centrifugation at 100 000 *g* for 1 h. FimD was primarily in the soluble fraction which was passed over a HiTrap Column (Pharmacia) charged with Ni^{2+} following the manufacturer's protocols. FimD was eluted in 20 mM HEPES (pH 7.5), 20 mM EDTA, 0.1% Elugent, 500 mM NaCl and desalted in a Centricon 30 (Amicon) to 20 mM HEPES (pH 7.5), 0.1% Elugent, 75 mM NaCl. Variations on the purification included using Tris instead of HEPES and Zwittergent 3-14 (Calbiochem) instead of Elugent.

Combinations of the different plasmids (pETS1, pETS2A, pETS5, pHJ20) and pETS1000 were transformed into ORN103 and protein production induced at OD_{600} ~0.6 by adding 0.05% arabinose (for FimC) and 500 μM IPTG (for the subunits) for 1 h at 37°C. Cells were harvested by centrifugation and periplasmic preparations were done following published protocols (Jones *et al.*, 1993). The various chaperone–subunit complexes were purified by Ni^{2+} chromatography using Ni-NTA–agarose beads (Qiagen) following the manufacturer's protocols with the following exceptions: 20 mM Tris (pH 8.0) was used to wash beads, and proteins were eluted in 20 mM Tris (pH 7.5) and 0.1 M EDTA. FimCA and FimCG complexes were dialyzed into 20 mM Tris (pH 8.0), and excess FimC was removed on a Mono-Q column using FPLC (Pharmacia). FimCH and FimCF complexes were dialyzed into 20 mM KMES (pH 6.5), and excess FimC was removed on a Mono-S column using FPLC (Pharmacia). All complexes were then placed into 10 mM HEPES (pH 7.5), 150 mM NaCl by buffer exchange in a Centricon 10 (Amicon). Additional FimC, FimCH, PapD, PapDG and $PapDA_{G150T}$ complexes were purified using protocols described previously (Jones *et al.*, 1993; Bullitt *et al.*, 1996). FPLC gel filtration chromatography was done on the FimD–C–H complex using a Superdex 200 column (Pharmacia) under the following buffer conditions: 20 mM Tris (pH 8.0), 100 mM NaCl, 0.5% Elugent.

Electrophoresis and Western blotting

SDS–PAGE was done using standard laboratory protocols. For Western (immuno) blotting, proteins were transferred to PVDF (Biorad) or nitrocellulose (Schleicher & Schuel) and blocked overnight in TBS (150 mM NaCl, 10 mM Tris–HCl, pH 7.5)/3% bovine serum albumin (BSA). Blots were washed three times with TBST (500 mM NaCl, 0.05% Tween-20, 20 mM Tris–HCl, pH 7.5), incubated with the appropriate antibody (anti-FimD and anti-FimCH were graciously provided by Medimmune Inc.) for 45 min, washed three times for 5 min with TBST, incubated with the secondary antibody [goat α-mouse or rabbit IgG-alkaline phoshatase (AP) conjugate (Pierce)], washed three times with TBST, and once with developer buffer (100 mM NaCl, 5 mM MgCl, 100 mM Tris–HCl, pH 9.5). The blots were developed in developer buffer with 0.04% NBT and 0.02% BCIP (Sigma).

ELISA

Briefly, purified FimD was allowed to adhere to microtiter plate wells overnight at 4°C in phosphate-buffered saline (PBS). Following washing with PBS and a 2 h blocking procedure, the various combinations of purified FimC–subunit complexes (or FimC alone) were incubated at room temperature in the wells for 1 h. After washing, a 1:1000 dilution of anti-FimC antibody was incubated in the wells for 45min. Following another washing, anti-rabbit IgG–AP conjugate (Sigma) was incubated for 45 min. Finally, after additional washing, *p*-nitrophenol phosphate was added. The OD_{405} was read after 1 h on a microtiter plate reader. Background absorbance and non-specific chaperone–subunit binding to the plate were subtracted out using negative controls of FimD alone and the various chaperone–subunit complexes alone.

Trypsin experiments

ORN103 cells were transformed with plasmids coding for FimD (pETS4), FimD together with combinations of the chaperone (FimC) and the various type 1 subunits (pETS1001, pETS1002, pETS1003, pETS1004, pETS1005) or FimC alone (pETS1000). Negative controls were included with vector only (pMMB66). FimD production from the cells growing at 37°C was induced at OD_{600} ~0.6 by addition of IPTG, and chaperone or chaperone–subunit complex production was induced by addition of arabinose. After 1 h, the cells were washed once with 20 mM HEPES (pH 7.5) and resuspended in 20 mM HEPES (pH 8.5). The resuspended cells were split into two equal portions. One half was digested with fresh 100 μg/ml trypsin (Sigma), and the other half mock digested (only the trypsin buffer was added). All were rocked at 37°C for 2 h. Then 10 mM phenylmethylsulfonyl fluoride (PMSF) was added, followed by harvesting by centrifugation, resuspending in HEPES and disruption by French Press. The outer membranes were isolated either by step sucrose gradient centrifugation (Nikaido, 1994) or by differential solublization (as described above for FimD purification). Outer membranes were isolated identically when using any of the type 1 pilus-producing strains; however, the cells were grown in static broth with passages as described previously (Jones *et al.*, 1995) until the bacteria gave an HA titer of 1:128. Protein sequencing was done by David McCourt at Midwest Analytical.

Biacore experiments

The Biacore 2000 machine, CM5 or NTA sensor chips and analysis programs were all from Pharmacia Biosensor. The detection principle for the Biacore is based on surface plasmon resonance (Karlsson *et al.*, 1991). One of the proteins (the ligand) is immobilized on the surface of the analysis chip (Johnsson *et al.*, 1991) and the other component (the analyte) is passed over this surface in a continuous flow. Binding of the analyte to the ligand results in a refractive index change near the surface, causing a change in the angle of light that is reflected off the gold-linked dextran matrix upon which the ligand is immobilized. This change is proportional to the increase in mass and is converted to response units (RU) and plotted on an axis versus time in a graph called a sensorgram (Fagerstam *et al.*, 1992) (see Figure 4A).

A sensorgram usually consists of an association phase when the analyte is first injected over the ligand surface, and a dissociation phase when the analyte is dissociating from the ligand and only buffer is flowing over the surface. The buffer used for the binding studies was 10 mM HEPES pH 7.5, 150 mM NaCl, 50 μM EDTA, 0.5% Elugent (Calbiochem). The kinetic association rate constant (k_{on}) and kinetic dissociation rate constant (k_{off}) can be calculated by direct analysis of the association and dissociation phase respectively, or by linear regression analysis. In order to minimize model fit or constant calculation errors due to analyte exhaustion (important in k_{on} calculations) or substrate rebinding (important during k_{off} calculations), the data actually used for determination of constants only represented 40 s—starting from 12 s following initiation of association/dissociation and continuing to the 52 s point. A lag of 12 s was used to allow detector stabilization following the bulk refractive index changes that occur with the injection of analyte (association) or buffer only (dissociation). All of the kinetic analyses assumed a pseudo-first order interaction between the immobilized ligand and the analyte. Model fits were superior using linear, single-site interaction models instead of non-linear, multi-site interaction methods of data evaluation based on χ^2, standard error and residual values, and

baseline offsets (as discussed in BIA Evaluation materials). Measured kinetic constant values were well within the range considered accurate for the Biacore 2000 machine and the BIA Evaluation software.

The K_D standard error values were calculated by averaging the standard errors from all of the k_{on} and k_{off} values for a particular chaperone–subunit complex and performing a division of standard errors calculation. Results in Figure 4A–D are from experiments on a CM5 chip; however, identical experiments done using an NTA chip (which immobilized FimD or PapC via the His tag) and non-His-tagged FimC, FimCH, PapD and PapDG gave essentially identical results (data not shown). All of the calculations and graphic analyses were done using the equations provided in the BIA Evaluation software package.

Acknowledgements

We would like to thank Dr R.John Collier for allowing much of this work to be physically undertaken in his laboratory. Additionally, we thank Dr R.John Collier, the members of the Collier lab and Dr C.Hal Jones for many helpful discussions. This work was supported by National Institutes of Health grants R01AI29549 and R01DK51406.

References

Bitter,W., Koster,M., Latijnhouwers,M., de Cock,H. and Tommassen,J. (1998) Formation of oligomeric rings by XcpQ and PilQ, which are involved in protein translocation across the outer membrane of *Pseudomonas aeruginosa*. *Mol. Microbiol.*, **27**, 209–220.

Bullitt,E., Jones,C.H., Striker,R., Soto,G., Jacob-Dubuisson,F., Pinkner,J., Wick,M.J., Makowski,L. and Hultgren,S.J. (1996) Development of pilus organelle subassemblies *in vitro* depends on chaperone uncapping of a beta zipper. *Proc. Natl Acad. Sci. USA*, **93**, 12890–12895.

Connell,H., Agace,W., Klemm,P., Schembri,M., Marild,S. and Svanborg,C. (1996) Type 1 fimbrial expression enhances *Escherichia coli* virulence for the urinary tract. *Proc. Natl Acad. Sci. USA*, **93**, 9827–9832.

Dodson,K.W., Jacob-Dubuisson,F., Striker,R.T. and Hultgren,S.J. (1993) Outer membrane PapC usher discriminately recognizes periplasmic chaperone–pilus subunit complexes. *Proc. Natl Acad. Sci. USA*, **90**, 3670–3674.

Fagerstam,L.G., Frostell-Karlsson,A., Karlsson,R., Persson,B. and Ronnberg,I. (1992) Biospecific interaction analysis using surface plasmon resonance detection applied to kinetic, binding site, and concentration analysis. *J. Chromatogr.*, **597**, 397–410.

Furste,J., Pansegrau,W., Frank,R., Blocker,H., Scholz,P., Bagdasarian,M. and Lanka,E. (1986) Molecular cloning of the plasmid RP4 primase region in a multi-host-range tacP expression vector. *Gene*, **48**, 119–131.

Holmgren,A. and Brändén,C.-I. (1989) Crystal structure of chaperone protein PapD reveals an immunoglobulin fold. *Nature*, **342**, 248–251.

Hull,R.A., Gill,R.E., Hsu,P., Minshaw,B.H. and Falkow,S. (1981) Construction and expression of recombinant plasmids encoding type 1 and D-mannose-resistant pili from a urinary tract infection *Escherichia coli* isolate. *Infect. Immun.*, **33**, 933–938.

Hultgren,S.J., Schwan,W.R., Schaeffer,A.J. and Duncan,J.L. (1986) Regulation of production of type 1 pili among urinary tract isolates of *Escherichia coli*. *Infect. Immun.*, **54**, 613–620.

Hultgren,S.J., Jones,C.H. and Normark,S. (1996) Bacterial adhesins and their assembly. In Neidhardt,F.C. (eds), *Escherichia coli and Salmonella.* ASM Press, Washington, DC, pp. 2730–2757.

Hung,D., Knight,S., Woods,R., Pinkner,J. and Hultgren,S.J. (1996) Molecular basis of two subfamilies of immunoglobulin-like chaperones. *EMBO J.*, **15**, 3792–3805.

Jacob-Dubuisson,F., Striker,R. and Hultgren,S.J. (1994) Chaperone-assisted self-assembly of pili independent of cellular energy. *J. Biol. Chem.*, **269**, 12447–12455.

Johnsson,B., Lofas,S. and Lindquist,G. (1991) Immobilization of proteins to a carboxymethyldextran-modified gold surface for biospecific interaction analysis in surface plasmon resonance sensors. *Anal. Biochem.*, **198**, 268–277.

Jones,C.H., Pinkner,J.S., Nicholes,A.V., Slonim,L.N., Abraham,S.N. and Hultgren,S.J. (1993) FimC is a periplasmic PapD-like chaperone that directs assembly of type 1 pili in bacteria. *Proc. Natl Acad. Sci. USA*, **90**, 8397–8401.

Jones,C.H., Pinkner,J.S., Roth,R., Heuser,J., Nicholes,A.V., Abraham,S.N. and Hultgren,S.J. (1995) FimH adhesin of type 1 pili is assembled into a fibrillar tip structure is the Enterobacteriaceae. *Proc. Natl Acad. Sci. USA*, **92**, 2081–2085.

Jones,C.H., Danese,P., Pinkner,J., Silhavy,T. and Hultgren,S.J. (1997) Chaperone-assisted membrane release and folding pathway sensed by two signal transduction systems. *EMBO J.*, **16**, 6394–6406.

Karlsson,R., Michaelsson,A. and Mattsson,L. (1991) Kinetic analysis of monoclonal antibody–antigen interactions with a new Biosensor based analytical system. *J. Immunol. Methods*, **145**, 229–240.

Kazmierczak,B., Mielke,D., Russel,M. and Model,P. (1994) pIV, a filamentous phage protein that mediates phage export across the bacterial cell envelope, forms a multimer. *J. Mol. Biol.*, **238**, 187–198.

Klemm,P. and Christiansen,G. (1987) Three *fim* genes required for the regulation of length and mediation of adhesion of *Escherichia coli* type 1 fimbrae. *Mol. Gen. Genet.*, **208**, 439–445.

Klemm,P. and Christiansen,G. (1990) The *fimD* gene required for cell surface localization of *Escherichia coli* type 1 fimbriae. *Mol. Gen. Genet.*, **220**, 334–338.

Krogfelt,K.A., Bergmans,H. and Klemm,P. (1990) Direct evidence that the FimH protein is the mannose specific adhesin of *Escherichia coli* type 1 fimbriae. *Infect. Immun.*, **58**, 1995–1999.

Kuehn,M.J., Ogg,D.J., Kihlberg,J., Slonim,L.N., Flemmer,K., Bergfors,T. and Hultgren,S.J. (1993) Structural basis of pilus subunit recognition by the PapD chaperone. *Science*, **262**, 1234–1241.

Langermann,S. *et al.* (1997) Prevention of mucosal *Escherichia coli* infection by FimH–adhesin-based systemic vaccination. *Science*, **276**, 607–611.

Lee,C. (1997) Type III secretion systems: machines to deliver bacterial proteins into eukaryotic cells? *Trends Microbiol.*, **5**, 148–156.

Linderoth,N., Simon,M. and Russel,M. (1997) The filamentous phage pIV multimer visualized by scanning transmission electron microscopy. *Science*, **278**, 1635–1637.

Maurer,L. and Orndorff,P.E. (1985) A new locus, *pilE*, required for the binding of type 1 piliated *Escherichia coli* to erythrocytes. *FEMS Microbiol. Lett.*, **30**, 59–66.

Minion,F.C., Abraham,S.N., Beachey,E.H. and Goguen,J.D. (1989) The genetic determinant of adhesive function in type 1 fimbriae of *Escherichia coli* is distinct from the gene encoding the fimbrial subunit. *J. Bacteriol.*, **165**, 1033–1036.

Mitsui,Y., Dyer,F.P. and Langridge,R. (1973) X-ray diffraction studies on bacterial pili. *J. Mol. Biol.*, **79**, 57.

Nikaido,H. (1994) Isolation of outer membranes. *Methods Enzymol.*, **235**, 225–234.

Orndorff,P.E. and Falkow,S. (1984) Organization and expression of genes responsible for type 1 piliation in *Escherichia coli*. *J. Bacteriol.*, **159**, 736–744.

Roberts,J.A. *et al.* (1994) The Gal α(1–4) Gal-specific tip adhesin of *Escherichia coli* P-fimbriae is needed for pyelonephritis to occur in the normal urinary tract. *Proc. Natl Acad. Sci. USA*, **91**, 11889–11893.

Russel,M. (1995) Moving through the membrane with filamentous phages. *Trends Microbiol.*, **3**, 223–228.

Russell,P.W. and Orndorff,P.E. (1992) Lesions in two *Escherichia coli* type 1 pilus genes alter pilus number and length without affecting receptor binding. *J. Bacteriol.*, **174**, 5923–5935.

Salmond,G. (1996) Pili, peptidases, and protein secretion: curious connections. *Trends Microbiol.*, **4**, 474–476.

Thanassi,D.G., Saulino,E.T., Lombardo,M.-J., Roth,R., Heuser,J. and Hultgren,S.J. (1998) The PapC usher forms an oligomeric channel: implications for pilus biogenesis across the outer membrane. *Proc. Natl Acad. Sci. USA*, **95**, 3146–3151.

Valent,Q.A., Zaal,J., Degraaf,F.K. and Oudega,B. (1995) Subcellular localization and topology of the K88 usher FaeD in *Escherichia coli*. *Mol. Microbiol.*, **16**, 1243–1257.

Received November 26, 1997; revised and accepted February 16, 1998